# Effect of shape and surface chemistry of TiO$_2$ colloidal nanocrystals on the organic vapor absorption capacity of TiO$_2$/PMMA composite

Annalisa Convertino [a,*], Gabriella Leo [a], Marinella Striccoli [b], Gaetano Di Marco [c], M. Lucia Curri [b]

[a] Dipartimento di Progettazione Molecolare, C.N.R., Istituto per lo Studio dei Materiali Nanostrutturati, via Salaria km. 29.300, 00016 Monterotondo St., Roma, Italy
[b] Dipartimento di Materiali e Dispositivi, C.N.R., Istituto per i Processi Chimici e Fisici, Bari Division via Orabona 4, 70126 Bari, Italy
[c] Dipartimento di Materiali e Dispositivi, C.N.R., Istituto per i Processi Chimici e Fisici, Messina Division, C.da Papardo, Salita Sperone, 98158 Messina, Italy

## ABSTRACT

The organic vapor absorption capacity of poly(methyl metacrylate) (PMMA), filled with oleic acid (OLEA) capped TiO$_2$ nanocrystals (NCs) with curved shape, rod-like and spherical, is studied. The NC shape combined with the nature of the capping molecules can be used to enhance or reduce the PMMA ability to absorb different solvent molecules in a controlled way. Indeed, the arrangement of the ligands at the NC surface demonstrates an effective tool to control the extent of the interaction between the penetrating molecules and the embedded NCs from the outer to the inner specific chemical functionality of the coordinating ligand molecules.

© 2008 Elsevier Ltd. All rights reserved.

## 1. Introduction

Polymer networks exposed to solvent vapors absorb the organic molecules and swell to an equilibrium state, where the tendency to absorb solvent molecules is balanced by the elastic response of the network [1]. After desorbing the solvent molecules, the polymer then shrinks and returns to its initial volume. The swelling and shrinking properties of polymers are currently being exploited in a large number of important industrial applications including chemical sensing [2–5], controlled drug delivery [6], muscle-like actuators [7], and metal extraction and separation applications [8]. On the other hand, in many technological fields the swelling is considered detrimental and needs to be avoided. Indeed, the penetration of molecules from outer environment into polymers can have disastrous effects, as in the case of water or gases molecules diffusion into food and beverage packaging. In this scenario the ability to enhance or reduce/inhibit the gas or vapor diffusion into a polymer material, according to the needs of the final applications, would have tremendous technological fallout.

Recent studies have shown that the ability of a polymer to absorb solvent molecules can be modified by filling the polymer with inorganic nanoparticles [9–15]. In particular, the interaction between the active sites on the surface of the nanoparticles and the penetrating molecules can control the selectivity, rate and efficiency of the absorption capability of the host polymer, thus offering a powerful tool to quantitatively vary the swelling/shrinking behavior in the polymer composite.

In this perspective curved nanofillers, rod-like and sphere shaped, present specific advantages due to their high surface-to-volume ratio, which can dramatically increase the number of active sites available for interaction with analyte molecules. Furthermore the use of colloidal nanocrystals (NCs) as nanofillers would offer further remarkable advantages afforded by the ease in both manipulating the shape and tailoring the chemical characteristics of the surface by using versatile functional groups, including biocompatible ones, able to effectively and selectively interact with different analytes.

In this work, we highlight on how the shape, rod-like or spherical, combined with surface chemical properties of the nanofillers can influence the swelling behavior of a polymer. This is a fundamental technical issue that needs to be fully clarified for possible exploitation of the potential offered by polymer composites for suitably controlled vapor/gas absorption properties as well as for all those applications where the interaction between capped nanoparticles and analyte molecules plays a fundamental role.

Here we demonstrate that the dispersion of TiO$_2$ colloidal NCs, capped by oleic acid (OLEA), in poly(methyl metacrylate) (PMMA) results in a degree of swelling upon exposure to the same solvent, that can be increased or reduced by simply varying the geometry,

* Corresponding author. Tel.: +39 06 90672345; fax: +39 06 90672839.
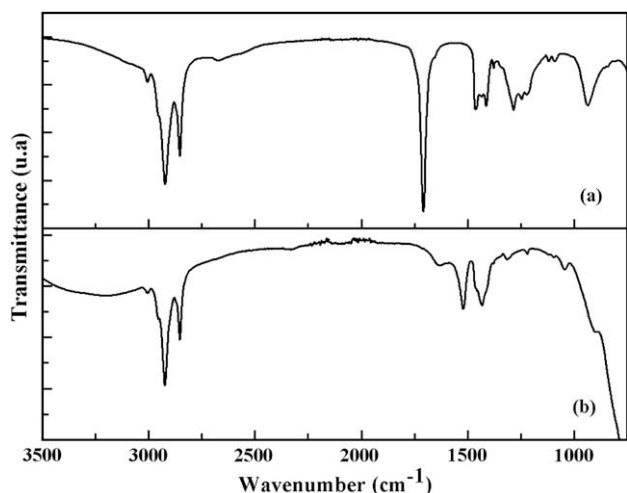  *E-mail address:* annalisa.convertino@ismn.cnr.it (A. Convertino).

**Fig. 1.** FT-IR spectra in the 3500–400 cm$^{-1}$ region of: (a) OLEA and (b) OLEA capped TiO$_2$ nanorods.

rod-like or spherical, of the nanofiller involved. The comparison between spherical and rod shaped TiO$_2$ NCs has been made possible thanks to an effective colloidal synthetic route [16] that allows to manipulate the NC shape, providing gram-scale quantities of organic-capped spherical or rod shaped NCs dispersed in chloroform solution by simply controlling the NC growth kinetics.

The swelling of the PMMA nanocomposite films was investigated at room temperature by measuring vis–IR reflectance spectra of the samples, deposited on Si substrates, in the presence of solvent vapors. Different solvents, like acetone, ethanol, propan-2-ol and water, were carefully chosen for their difference in polarity, number of C–H bonds, and pure PMMA swelling ability.

Then the swelling results were related to atomic force microscopy (AFM) observations and glass transition temperature, $T_g$, measurements performed on the PMMA nanocomposite samples to clarify fully the critical role played by the nanoscale curvature and the organic capping of the fillers in controlling the absorption capacity of the host polymer.

## 2. Experimental section

Titanium tetraisopropoxide (Ti(OPr$^i$)$_4$ or TTIP, 99.999%), trimethylamino-$N$-oxide dihydrate ((CH$_3$)$_3$NO·2H$_2$O or TMAO, 98%, water solution), anhydrous ethyleneglycol (HO(CH$_2$)$_2$OH or EG, 99.8%), and oleic acid (C$_{18}$H$_{33}$CO$_2$H or OLEA, 90%) were purchased from Aldrich and were used as-received without further purification or distillation. All solvents used were of analytical grade and purchased from Aldrich.

Organic-capped anatase TiO$_2$ NCs were synthesized by hydrolysis of TTIP using technical grade OLEA as surfactant at low temperatures (80–100 °C) [16]. Briefly, hydrolysis of TTIP was carried out by an excess of aqueous base solution in the presence of TMAO as catalyst for polycondensation. The morphology of the resulting TiO$_2$ NCs was modulated by varying the rate of water supply in the reaction mixture. One-dimensional growth was guaranteed by direct injection of large aqueous base volumes in OLEA: TTIP mixtures, while nearly spherical particles were obtained upon in situ water release (from the slow esterification reaction of OLEA and added EG).

The extraction procedures were subsequently performed in air: TiO$_2$ NCs were readily precipitated upon addition of an excess of ethanol (or methanol) to the reaction mixture at room temperature. The resulting precipitate was isolated by centrifugation and repeatedly washed (three times) with ethanol to remove surfactant residuals. The resulting OLEA capped rod-like and dot-like TiO$_2$ NCs were homogeneously dispersed in chloroform solutions. By this way, highly concentrated transparent solution of TiO$_2$ NCs was obtained, stable over months.

Nanocomposite materials were prepared by incorporation of pre-made nanoparticles in organic polymers with the use of a common blending solvent by adding high molecular weight PMMA to a CHCl$_3$ solution of TiO$_2$ nanorods and nanospheres at increasing nanofillers concentration (from 0.025 M to 0.2 M), corresponding to an NC load percentage in polymer ranging from 4 wt% to 36 wt%. Prior to the incorporation, the NCs were repeatedly washed (three times) with ethanol to remove surfactant excess. A polymer concentration of 0.05 g/ml was selected to achieve optically clear nanocomposite solutions. The NC/polymer blend was gently stirred until the complete polymer dissolution in CHCl$_3$. Thin films were prepared depositing by spin-coating (using an EC101DT Photo Resist Spinners, Headway Research Inc.) few drops of the NC–polymer mixture onto properly cleaned glass and silicon substrates at 3000 rpm for 30 s. The film thickness, measured by means of Alpha-Step 500 surface profiler, was found in the range from 400 nm up to 1 μm, strongly depending on the NC concentration and surface ligand compositions.

Fourier transform infrared (FT-IR) spectroscopy was used to investigate the nature of the organic coating on the surface of the TiO$_2$ NCs. TiO$_2$ powders for FT-IR analysis were prepared by washing the extracted precipitate repeatedly (three times) in order to remove physisorbed surfactant molecules, and then evaporating the residual solvent under vacuum at room temperature.

In Fig. 1 the typical IR spectra in the region 3500–400 cm$^{-1}$ of the OLEA capped TiO$_2$ nanorods (Fig. 1b) are reported and compared with that of the pure acid (Fig. 1a). A similar spectrum was obtained for the OLEA capped TiO$_2$ dots. Above 2000 cm$^{-1}$ the
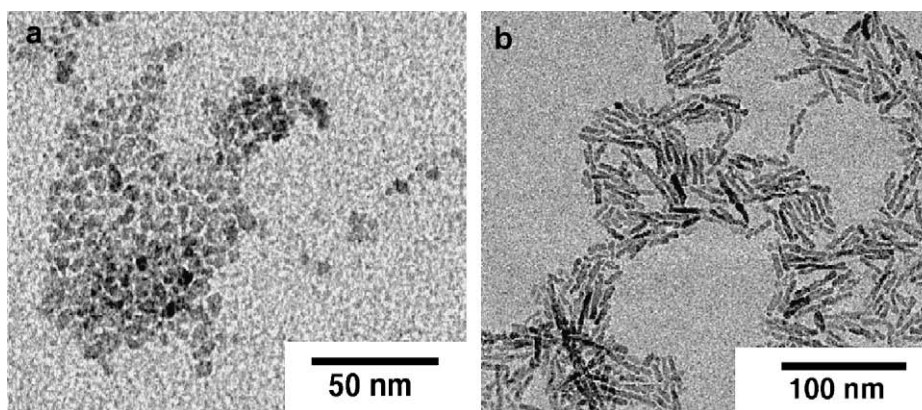


**Fig. 2.** TEM image of TiO$_2$ (a) nanospheres–PMMA nanocomposite and (b) nanorods–PMMA thin films deposited on a carbon-coated 400 mesh copper grids by spin coating.

TiO$_2$ sample (Fig. 1b) exhibits the intense antisymmetric and symmetric C–H stretching vibrations [17] (at 2920 and 2850 cm$^{-1}$, respectively) of the –CH$_2$– groups in the hydrocarbon moiety. The shoulder at 2960 cm$^{-1}$ can be associated with the asymmetric stretching of the terminal –CH$_3$ group of the alkyl chain. A weak but definite band at 3008 cm$^{-1}$, attributable to the olefinic C–H [17a], is also present in the OLEA capped TiO$_2$. Below 2000 cm$^{-1}$, the spectrum of the OLEA capped TiO$_2$ NCs shows the two characteristic bands centered at 1520 and 1436 cm$^{-1}$ related to the COO$^-$ antisymmetric and symmetric stretching vibrations of carboxylate anions complexed with surface Ti centers. The lack of clear evidence for the free C=O stretching band at around 1650–1720 cm$^{-1}$ (cf. 1775 cm$^{-1}$ for OLEA in the vapor phase) seems to exclude the presence of both un-ionized OLEA monomers and dimmers [17a,b] possibly having the C=O involved in H-bonding with a Ti-OH$_2^+$ surface group. Then the FT-IR analysis confirms the coordination behavior of the polar moiety of the fatty acid binding the NC surface atoms and the attachment of a monolayer of OLEA to the NC surface. The FT-IR analysis clearly shows the coordination

behavior of the polar moiety of the fatty acid binding the NC surface atoms.

Low resolution transmission electron microscopy (TEM) images were recorded using a Jeol Jem 1011 microscope operating at an accelerating voltage of 100 kV. TEM samples were prepared depositing one drop of nanocomposite solution onto a carbon-coated 400 mesh copper grids by spin coating at 6000 rpm. The content of NCs dispersed in PMMA was 80 wt%. The images in Fig. 1 show nanospheres (Fig. 2a) and nanorods (Fig. 2b) of 6 nm of diameter and 30 nm of average length.

The surface morphology and roughness of the as-prepared PMMA and PMMA composite films were investigated by atomic force microscopy (AFM) operating in air in tapping mode with a high resonance supersharp Si tip ($k = 30$ N/m, $f_0 = 300$ kHz) and Al coated Si tips ($k = 40$ N/m, $f_0 = 300 \pm 100$ kHz). For each sample, images were recorded from different positions and different scan sizes ranging from 1 μm × 1 μm to 50 μm × 50 μm in order to check the lateral uniformity of the TiO$_2$/PMMA thin films.
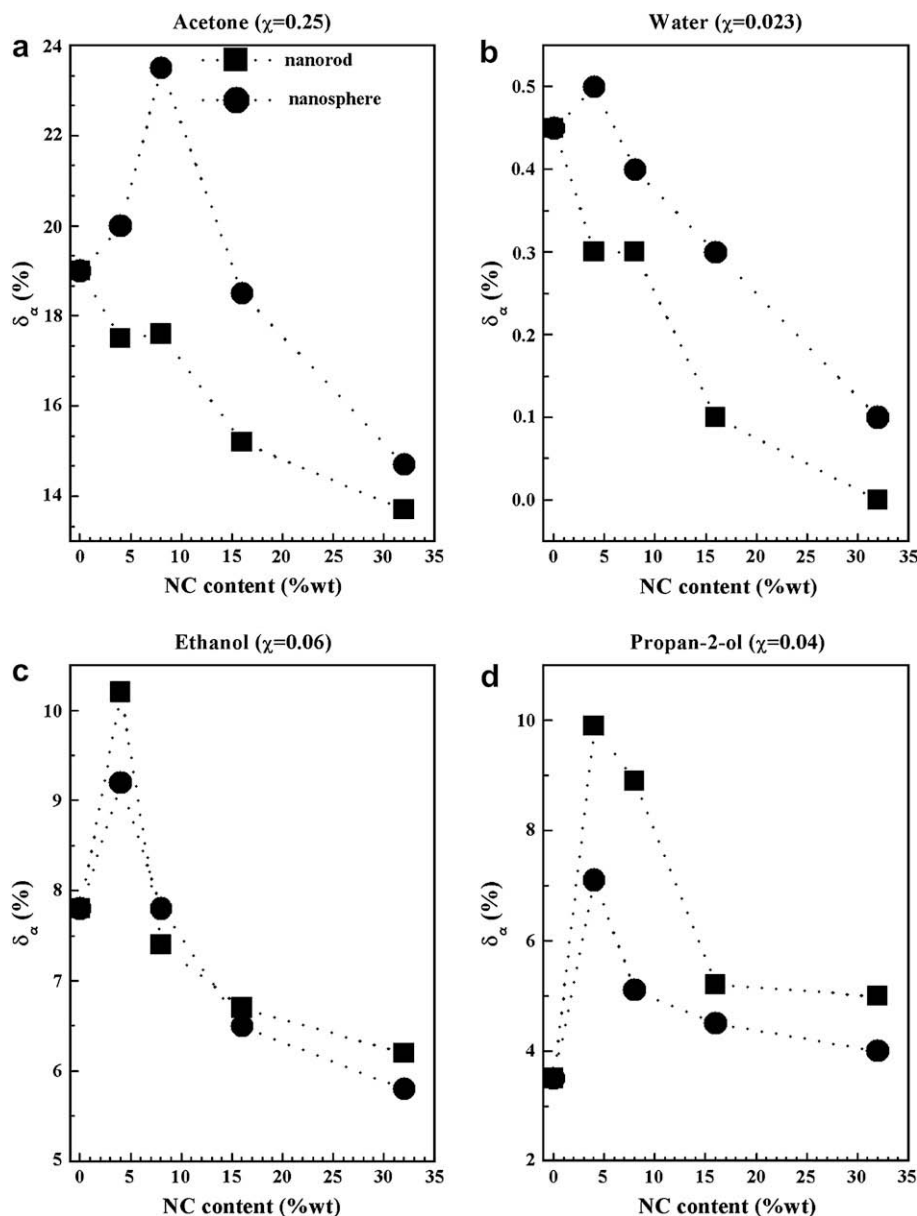


**Fig. 3.** Solvent uptake at the equilibrium, $\delta_\infty$, as a function of the TiO$_2$ loading in the case of spherical and rod-like nanofillers for the exposure to vapors of (a) acetone, (b) water, (c) ethanol, and (d) propan-2-ol alcohol. $\chi$ is the molar fraction of the vapor in air. The dotted lines are guide for the eye.

A dynamic mechanical thermal analyzer (DMTA) of the Polymer Laboratories was used to determine storage, $E'$, and loss, $E''$, modules or internal friction Q-1 ($=E''/E'$). All the samples were obtained by evaporating the solvent in air for 24 h and then dried under vacuum at the same temperature for two days. To improve the homogeneity, the as-prepared samples were compression molded between two disks of Teflon at a temperature of 100 °C for 1 h and then quickly cooled at room temperature. In this way we obtained rods with approximate size of $20 \times 10 \times 0.3$ mm. The measurements were carried out in the $-20/180$ °C temperature and 0.3–30 Hz frequency range at a heating rate of 2 °C/min. The analysis of the mechanical spectra revealed an α-relaxation which follows the variation of the glass transition temperature ($T_g$) with the spherical and rod-like nanofillers.

The swelling was investigated by measuring at room temperature the visible and infrared reflectance spectra of the samples deposited on Si substrates in the presence of the different solvent vapors: acetone, ethanol, propan-2-ol and water. These solvents were carefully chosen for their difference in polarity, number of C–H bonds, and pure PMMA swelling ability. The absorption of the solvent molecules causes an increasing of the film thickness and as a consequence a shift of the position of the maxima and minima in the reflectance pattern of the PMMA composite films. The reflectance spectra were performed using a Cary 5 UV–vis–NIR spectrophotometer arranged for experiments in the presence of gas or vapor. The samples were inserted into a glass tube through which flowed synthetic air (20.5% of volume O in N) as carrier gas with a flow of 200 sccm. The organic vapor was introduced by bubbling synthetic air through the organic liquid. A mass flow controller system was automatically directed by Omicron apparatus. A more detailed description of the swelling measurements is in Supplementary material.

## 3. Results and discussion

Fig. 3 shows the measured solvent uptake, $\delta_\infty$, at the equilibrium, i.e. at time $t = \infty$, as a function of the TiO$_2$ NC loadings in the case of spherical and rod-like nanofillers for the four vapors tested. The solvent uptake $\delta_t$ at time $t$, defined as follows:

$$\delta_t = (d_t - d_o) \times 100/d_o$$

where $d_o$, is the initial thickness of the unswollen film and $d_t$ that of the swollen sample at time $t$, was obtained by fitting the experimental reflectance spectra of the PMMA and PMMA composite films, deposited on Si substrates, before and after a time of exposure, $t$, to solvent vapors.

The numerical analysis of such spectra was performed by using the standard matrix method [18]. The theoretical curves were obtained by using the optical constants measured on reference samples deposited onto quartz substrate [12] and assuming that the absorption of the solvent vapors produces negligible variation of refractive index of the PMMA and PMMA nanocomposite [19]. In Fig. 3 we observe a general enhancement of solvent uptake in composites at lower TiO$_2$ loadings ($\leq$8 wt%) in comparison with the pure PMMA (0 wt%). Only for PMMA composite filled with rod-like NCs in the presence of the polar solvents, water and acetone, the outcome is quite different; we indeed observe an immediate decrease in $\delta_\infty$ even at low loadings of TiO$_2$. Further additions of TiO$_2$ NCs, sphere or rod shaped, decrease the $\delta_\infty$ values, as has been already observed in the literature for similar polymer composites [20]. We attribute this behavior observed for NC loadings higher than 8 wt% to three different occurring events: (a) the reduction of the organic component in the nanocomposites which is the part of this hybrid system able to absorb solvent molecules, (b) the increasing of the inorganic part, which limits the ability of polymer

chains to move and to accommodate solvent molecules, (c) possible aggregation phenomena of the nanofillers, which cause a reduction of the sites available for the interaction with the penetrating molecules as it is explained in the following.

To quantify better the variation of the PMMA absorption capacity induced by the fillers in the dilute case (NC content $\leq$8 wt%) we plot in Fig. 4 the histogram of the relative variation of $\delta_\infty$, given in Fig. 3, of the PMMA nanocomposites with respect to that of the pure PMMA, $(\delta_{TiO_2/PMMA} - \delta_{PMMA})/\delta_{PMMA}$, for both rod and sphere shaped fillers, at the fixed NC content of 4 wt%, as a function of the different solvents investigated.

The general trend indicates that films with TiO$_2$ nanospheres possess an enhanced response to the polar solvents, acetone and water, as compared to those with TiO$_2$ nanorods, which instead lower the absorption capacity of the PMMA toward the same polar solvents. The exposure to weakly polar solvents, such as ethanol and propan-2-ol, causes an increasing swelling in the PMMA filled with both sphere and rod shaped NCs, but a better response is evident for nanorod fillers than for spherical ones. Remarkably, an original response was noticed for the exposure of the PMMA nanocomposites to propan-2-ol, which is generally considered a "poor" solvent for the swelling of bare PMMA. An impressive increase in PMMA swelling was indeed observed to occur for both nanorod and nanosphere inclusions, making thus the propan-2-ol a "good" solvent for the PMMA composite. Hence, Fig. 4 unequivocally demonstrates that the presence of organic-capped NCs at low loadings in PMMA matrix can enhance or reduce the process of solvent absorption in the matrix.

Fig. 5 shows 2 μm × 2 μm tapping mode AFM plan view of 4 wt% TiO$_2$ nanosphere (Fig. 5a) and nanorod (Fig. 5b) PMMA composites. A typical AFM image of pure PMMA thin film is also reported for comparison (Fig. 5c). The AFM measurements were performed on as-prepared samples before their exposure to solvents. The analysis of the AFM images shows that the morphology and surface roughness depend on the NC shape. Anyway, neither pores nor holes are present on the surface of the pure PMMA and PMMA nanocomposite films. Hence the occurrence of porosity on the film surface cannot be invoked to explain the different swelling behaviors observed in the PMMA composites. In addition, structures compatible with the occurrence of few isolated aggregates can be observed superimposed to the overall morphology of the PMMA composite.

To provide more insight into the characteristics of the NC–polymer interface, the glass transition temperature, $T_g$, was
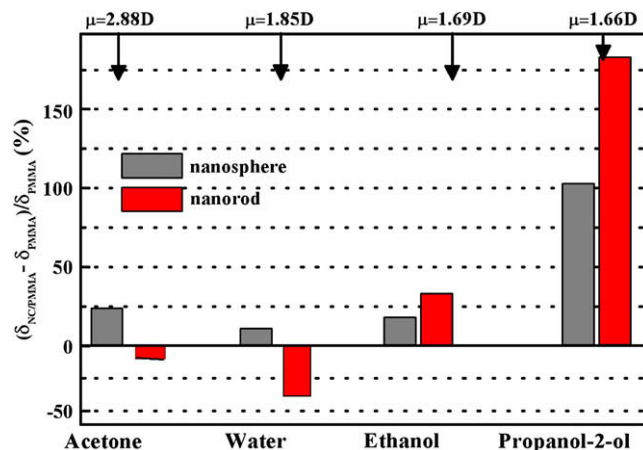
**Fig. 4.** Relative variation of solvent uptake at the equilibrium, $(\delta_{TiO_2/PMMA} - \delta_{PMMA})/\delta_{PMMA}$, for the PMMA composites with nanospheres and nanorods, at the fixed content of 4 wt%, as a function of the different solvents. $\mu$ is the electric dipole moment of the solvent molecule.
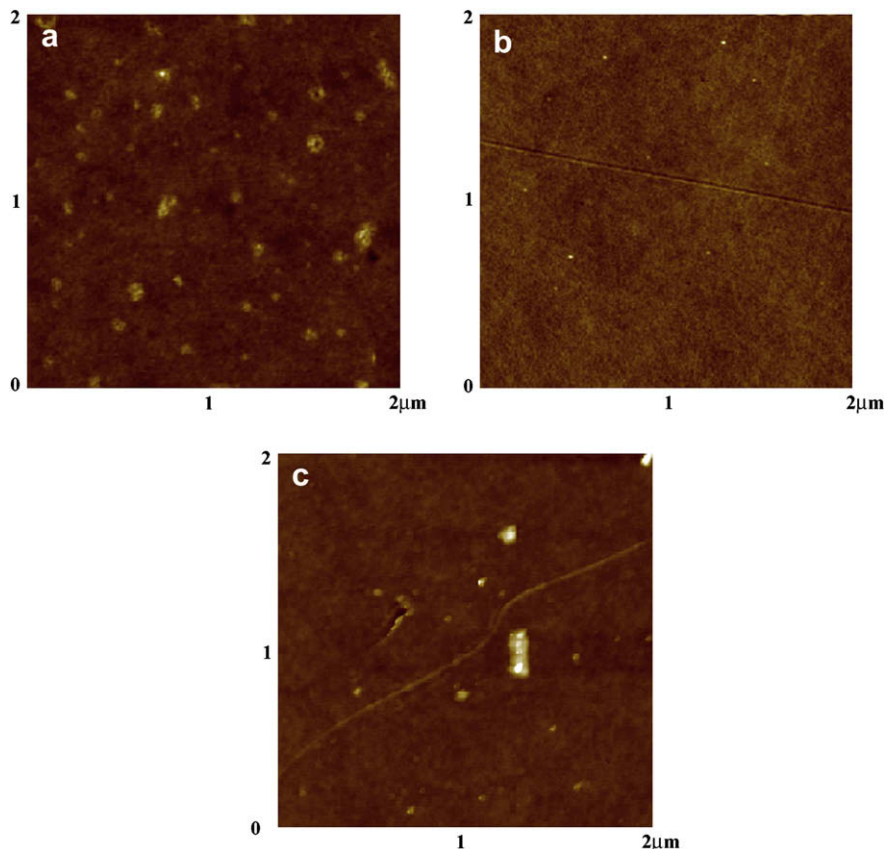
**Fig. 5.** 2 μm × 2 μm tapping mode AFM plan view of the nanocomposite thin films deposited on Si substrate: (a) 4 wt% TiO$_2$ nanosphere PMMA composite, z scale = 6 nm; (b) 4 wt% TiO$_2$ nanorod PMMA composite, z scale = 9 nm; (c) pure PMMA, z scale = 14 nm.

measured as a function of the NC content for both spherical and rod-like fillers. Fig. 6 shows a decrease of $T_g$ at low values of NC loadings with respect to the value found for the pure PMMA. The higher concentration of TiO$_2$ NCs reveals a $T_g$ value much higher than that obtained for the pure PMMA. This trend is typically found for all the investigated samples, irrespectively of the NCs shape. By focusing our attention on the behavior of the dilute case (≤8 wt%), the observed decrease of $T_g$ can be related, according to the most recent interpretation [21], to an increase of the polymer chain mobility in the vicinity of the fillers due to the presence of voids surrounding the NCs. These voids are formed because of a weak interaction of the polymer with the filler particle, which prevents the bonding of polymer segments on the NC surface.

The lowest value of $T_g$ observed at 4 wt% in the PMMA with nanospheres is due to the larger amount of interface area provided by the nanospheres with respect the nanorods [22].

According to these results the presence of free volume around the TiO$_2$ NCs should increase the swelling degree in the PMMA nanocomposites when exposed to the different solvent vapors irrespectively of the filler shape. Furthermore, we should expect a higher response toward all the investigated solvents by the spherical NC based PMMA composite than by the nanorod-based counterpart. Actually, Fig. 4 highlights two relevant features that are not in agreement with the above discussed conclusion: (a) the swelling degree induced by the polar solvents in the PMMA is increased in the presence of dots and is reduced by the rod inclusions and (b) larger swelling for exposure to the weakly polar solvents is observed in the PMMA filled with nanorods rather than in the spherical NC equivalent. This behavior unequivocally indicates that a different amount of voids inside the composite samples cannot account for the absorption capacity of the PMMA nanocomposite. The geometric characteristics of the NC surface

combined to its organic capping, i.e. the spatial arrangement of the capping molecules at the nanofiller surface, rather represents the key factor to understand the observed results.

The investigated OLEA capped nanofillers consist of nanosized titania cores terminating with an hydrocarbon periphery, as is illustrated in Fig. 7a and b, since a monolayer of OLEA molecules is co-ordinated, through their polar functional groups – $CO_2^-$, by means of a bidentate type of bonding to the metal atoms at the oxide surface, as reported in the literature [17] and confirmed by the FT-IR measurements. The sites, where the carboxyl group co-ordinate the metal atoms, together with the free Ti–O sites (not co-ordinated to any specific group) can be easily approached by the diffusing vapor
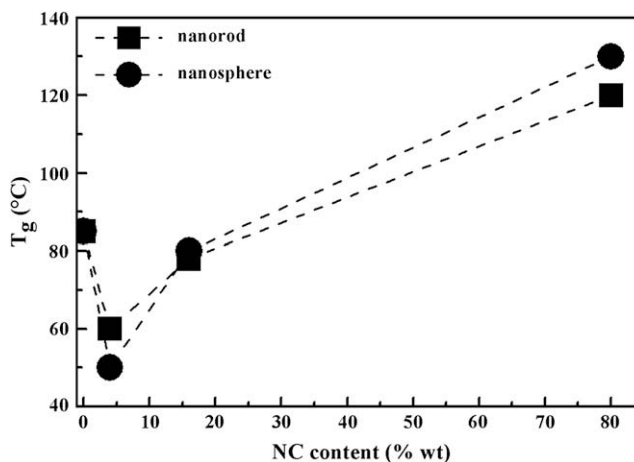


**Fig. 6.** $T_g$ of the PMMA nanocomposite as a function of the TiO$_2$ loading for spherical and rod-like nanofillers. The dotted lines are guide for eyes.
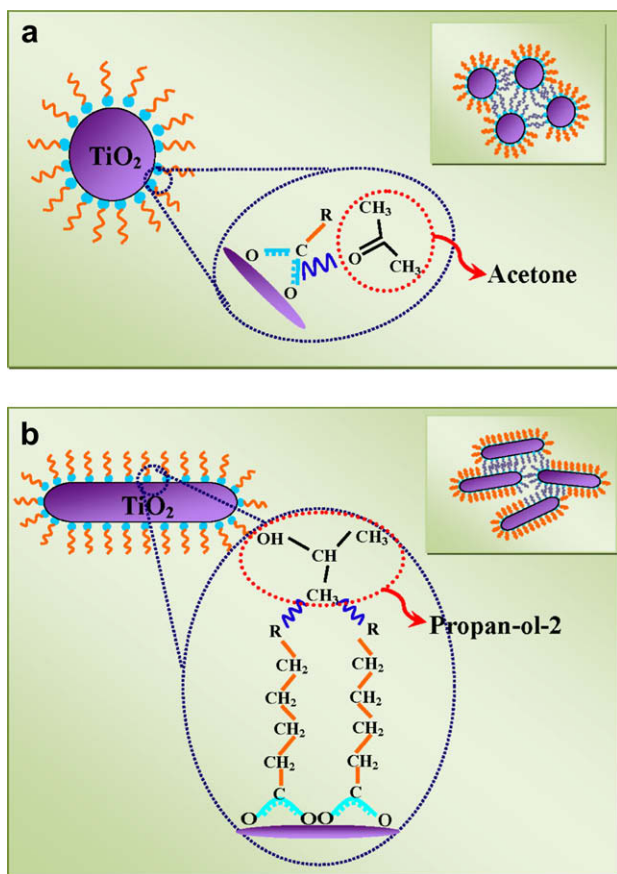
**Fig. 7.** Sketch of the interactions between the molecules of polar solvent (acetone) (a) and weak polar solvent (propan-2-ol) (b) with the OLEA capped nanosphere and nanorod, respectively.

molecules, due to the radial distribution of the OLEA molecules at the spherical surface of titania particle as sketched in Fig. 7a.

Due to their polar character, the carboxyl group and/or the Ti–O sites are more prone to efficiently interact with the solvent polar molecules via a strong dipole–dipole interaction, finally resulting in an increased sorption ability of the polymeric matrix toward acetone and water. In the case of the OLEA capped nanorods, the surface is less accessible for the polar molecules, being the capping molecules more densely packed than in the spherical particles (see sketch of nanorod in Fig. 7b). Such geometry results in a more efficient screening of the dipole–dipole interaction between solvent molecule and the polar bonds, carboxyl group of the OLEA and the free Ti–O sites, at the NC surface. In addition, the long apolar alkyl chain of the OLEA molecules presents a weak affinity for the polar solvents, especially for the water, thus causing a decrease of absorption capacity of the PMMA even with low NCs content for these solvents as evident in Fig. 4.

In agreement with this model, the increased absorption of propan-2-ol and ethanol in the PMMA composites, for both spherical and rod-like nanofillers, can be attributed to the affinity between aliphatic chains of the ligands and the C–H bonds in these solvents. The enhanced sensitivity of the PMMA toward the propan-2-ol can be ascribed to the larger number of C–H bonds in the propan-2-ol than in the ethanol. In this instance, the larger swelling observed for the rod-like fillers than for the nanospheres in the presence of weakly polar solvents can be ascribed to the fact that in the case of the nanospheres the polar bonds on the filler surface, carboxyl group of the OLEA and the free Ti–O sites, are not efficiently screened by aliphatic chains of OLEA. Then, the weak affinity between these surface polar bonds and the propan-2-ol and

ethanol occurs in competition with the interaction between OLEA aliphatic chains and the C–H bonds of these solvents, causing the smaller absorption capacity observed in PMMA with nanospheres when exposed to the weakly polar solvents with respect to the case of PMMA with nanorods.

It is worth to notice that at low content of NCs a certain degree of aggregation has to be taken into account, and as a consequence isolated NCs and some small aggregates could be dispersed in the PMMA matrix as evident in the AFM image (Fig. 5). Due to the protecting effect of the surface organic coating, the TiO$_2$ NCs in the polymer form close-packed aggregates [23] where each NC retains its individuality, as confirmed also by TEM images. Thus the OLEA molecules on the outer surface of these small aggregates continue to have a geometrical distribution characterized by the OLEA carboxyl groups and the free Ti–O sites ease to approach in the case of spherical LC aggregates and screened by the aliphatic chains of the OLEA in the rod-like NC aggregates (inset of Fig. 7a and b). Since the above-discussed hypothesis relies on the interaction between vapor and organic coated NC surface, they stand also in the presence of these small aggregated NCs, which may only turn into a slight reduction of the amount of sites available for absorption.

At NC content higher than 8 wt% the aggregation phenomena could cause a more relevant reduction of the amount of sites available for interaction with the penetrating molecules, thus contributing to induce the decrease in the swelling for composites having NC content higher than 8 wt%, irrespectively of the filler shape.

## 4. Conclusions

Inorganic-capped NCs dispersed in a polymer, at low loading, can control the absorption capacity of different solvents in the host polymer. The overall results demonstrate that the NC shape together with the nature of the capping molecules could be used for tuning the sensitivity of the polymer composite to a specific vapor composition. The distribution of the ligands at the NC surface can be effective to control the extent of the interaction between the penetrating molecules and the embedded NCs from the outer to the inner specific chemical functionality of the coordinating ligand molecules.

## Appendix. Supplementary material

Supplementary data associated with this article can be found in the online version at, doi: 10.1016/j.polymer.2008.09.069.

## References

[1] Flory PJ. Principles of polymer chemistry. Ithaca, NY: Cornell University Press; 1953 [chapter 13];
Treolar LRG. The physics of rubber elasticity. Oxford: Oxford University Press; 1975 [chapter 7];
Young RJ, Lovell PA. Introduction to polymers. London: Chapman & Hall; 1981;
Doyle FJ. In: Dusek K, editor. Advances in polymer sciences responsive gels: volume transitions, vols. I and II. Berlin: Springer; 1993.
[2] Potyrailo RA. Angew Chem Int Ed 2006;45(5):702–23;
Lang HP, Hegner M, Gerber C. Mater Today 2005;8(4):30–6.
[3] Lavrik NV, Sepaniak MJ, Datskos PG. Rev Sci Instrum 2004;75(7):2229–53.
[4] Grate JW. Chem Rev 2000;100(7):2627–48.
[5] (a) Convertino A, Capobianchi A, Valentini A, Cirillo ENM. Adv Mater 2003;15(13):1103–5;
(b) Palkovitos R, Mayer C, Bauer G, Winkler H, Pittner F, Schalkhammer T. Biopolymers 2003;69(3):333–42.

[6] Peppas NA, Bures P, Leobandung W, Ichikawa H. Eur J Pharm Biopharm 2000;50(1,3):27–46.

[7] (a) Shahinpoor M. J Intell Mater Syst Struct 1995;6(3):307–14;
(b) Shahinpoor M, Bar-Cohen Y, Simpson JO, Smith J. Smart Mater Struct 1998;7:R15–30.

[8] (a) Feil H, Bae YH, Feijen J, Kim SW. J Membr Sci 1991;64(3):283–94;
(b) Oren S, Caykara T, Kantoglu O, Guven O. J Appl Polym Sci 2000; 78(12):2219–26;
(c) Kasgoz H, Ozgumus S, Orbay M. Polymer 2003;44(6):1785–93;
(d) Zhang Qiu Gen, Liu Qing Lin, Lin Jie, Chen Jian Hua, Zhu Ai Mei. J Mater Chem 2007;17:4889–95.

[9] Convertino A, Valentini A, Bassi A, Cioffi N, Torsi L, Cirillo ENM. Appl Phys Lett 2002;80(9):1565–7.

[10] Gritsenko KP, Grynko DO, Capobianchi A, Convertino A, Friedrich J, Schulze RD, et al. In: Iwamori Satoru, editor. Polymer surface modification and polymer coatings by vacuum technology. Fort P.O., Trivandrum, Kerala, India: Research Signpost; 2005. p. 85–109.

[11] Haraguchi K, Takehisa T. Adv Mater 2002;14(16):1120–3.

[12] Convertino A, Leo G, Tamborra M, Sciancalepore C, Striccoli M, Curri ML, et al. Sensors Actuators B 2007;126(1):138–43.

[13] Vossmeyer T, Guse B, Besnard I, Bauer RE, Mullen K, Yasuda A. Adv Mater 2002;14(3):238–42.

[14] Potyrailo RA, Leach AM. Appl Phys Lett 2006;88(13):134110.

[15] Evans SD, Johnson SR, Cheng YL, Shen T. J Mater Chem 2000;10:183–8.

[16] Cozzoli PD, Kornowski A, Weller H. J Am Chem Soc 2003;125(47):14539–48.

[17] (a) Thistlethwaite PJ, Hook MS. Langmuir 2000;16(11):4993–8;
(b) Nara M, Torii H, Tasumi M. J Phys Chem 1996;100(51):19812–7;
(c) Thistlethwaite PJ, Gee ML, Wilson D. Langmuir 1996;12(26):6487–91.

[18] Born M, Wolf E. Principles of optics. New York: Pergamon; 1964. pp. 51–70.

[19] The change in refractive index of the PMMA matrix caused by the swelling follows from the Lorentz–Lorenz formula (in Ref. [17]). Assuming that the additional volume of the film was due to solvent uptake we have that the refractive index of the swollen film, $n_{tot}$, is $n_{tot} = \{[(n_1^2 \cdot X_1)/(n_1^2 + 2) + (n_2^2 \cdot X_2)/(n_2^2 + 2)]/[X1/(n_1^2 + 2) + X_2/(n_2^2 + 2)]\}^{1/2}$ where $X_1$ and $X_2$ are the volume fractions, and $n_1$ and $n_2$ are the bulk refractive indices of the PMMA ($n_1 = 1.54$ from reference sample) and the solvent. In: Weast RC, editor. Handbook of chemistry and physics. CRC Press; 1978–1979. respectively. For example, in the case of the acetone, which is the solvent inducing the highest degree of swelling, taking into account an amount of $X_2$ of 25%, we obtain a variation of the refractive index $\Delta n/n$ around 1%.

[20] (a) Brosseau C, Boulic F, Queffelec P, Bourbigot C, Le Mest Y, Loaec J, et al. J Appl Phys 1997;81(2):882–90;
(b) Bassi A, Valentini A, Convertino A. Appl Phys A 2000;71(1):109–11;
(c) Cioffi N, Farellab I, Torsi L, Valentini A, Sabbatini L, Zambonin PG. Sens Actuators B 2003;93(1–3):181–6.

[21] (a) Bansal A, Yang H, Li C, Cho K, Benicewicz BC, Kumar SK, et al. Nat Mater 2005;4(9):693–8;
(b) Schadler LS, Kumar SK, Benicewicz BC, Lewis SL, Harton SE. MRS Bull 2007;32(4):335–40;
(c) Ash BJ, Schadler LS, Siegel RW. Mater Lett 2002;55(1–2):83–7.

[22] In the approximation of isolated nanofillers with spherical or rod-like shape, the total absorption surface area of the embedded fillers is $S = ns = (V/v) \cdot s$. Where $n$ is the total number of nanofillers, $V$ is the volume fraction of the inorganic component, $v$ and $s$ are the volume and surface of the isolated nanofiller, respectively. Because in our samples the radius, $r$, of the nanospheres and the nanorods is the same, the ratio between the total surface area of the nanospheres, $S_{sphere}$, and that of the nanorods, $S_{rod}$, at a fixed mass fraction, i.e. the same $V$, is $S_{sphere}/S_{rod} = (s_{sphere}/v_{sphere}) \cdot (v_{rol}/s_{rod}) = 3h/2(r + h)$ where $h$ is the height of the rods. By considering the values of $r$ and $h$ estimated by TEM images, we have $S_{sphere}/S_{rod} \approx 1.4$.

[23] Sciancalepore C, Cassano T, Curri ML, Mecerreyes D, Valentini A, Agostiano A, et al. Nanotechnology 2008;19:205705–13.